



Semnan University



Research Article

## Magnetic Nanoadsorbent: Preparation, characterization, and Adsorption Properties for Removal of Copper(II) from Aqueous Solutions

Mohsen Esmailpour\*<sup>ORCID</sup>, Majid Ghahraman Afshar\*<sup>ORCID</sup>

Chemistry and Process Research Department, Niroy Research Institute (NRI), Tehran, Iran

### PAPER INFO

*Article history:*

Received: 29/Aug/2022

Revised: 08/Nov/2022

Accepted: 15/Nov/2022

### Keywords:

Fe<sub>3</sub>O<sub>4</sub>@SiO<sub>2</sub> NPs; Bis-salophen Schiff base ligand; Adsorption kinetics; Copper ions; Magnetic separation

### ABSTRACT

A novel, bis-salophen schiff base ligand anchored magnetic Fe<sub>3</sub>O<sub>4</sub>@SiO<sub>2</sub> nanoparticles was prepared and applied for removal of Cu(II) from aqueous solutions. The obtained Fe<sub>3</sub>O<sub>4</sub>@SiO<sub>2</sub>/Schiff base MNPs was characterized by fourier transform infrared (FT-IR), X-ray diffraction (XRD), transmission electron microscopy (TEM), field emission scanning electron microscopy (FE-SEM), energy dispersive X-ray analysis (EDX) and vibration sample magnetometry (VSM). Then, the adsorption activity for copper ions was studied by nonmagnetic, in terms of effect of adsorbent dosage on the adsorption and kinetics behavior. Furthermore, the adsorption and regeneration experiment showed there was about 5% loss in the adsorption capacity of the prepared Fe<sub>3</sub>O<sub>4</sub>@SiO<sub>2</sub>/Schiff base MNPs for copper ions after 6 times reuse. Finally, our results suggested that the Fe<sub>3</sub>O<sub>4</sub>@SiO<sub>2</sub>/Schiff base composites have a great potential to be employed for treatment of wastewater containing Cu(II).

DOI: <https://doi.org/10.22075/CHEM.2023.28238.2095>

This is an open access article under the CC-BY-SA 4.0 license. (<https://creativecommons.org/licenses/by-sa/4.0/>)

\*.Corresponding author: Assistant Professor of Chemistry, Chemistry and Process Research Department, Niroy Research Institute (NRI), Tehran, Iran. E-mail address: [mesmaeilpour@nri.ac.ir](mailto:mesmaeilpour@nri.ac.ir) & [mghahramanafshar@nri.ac.ir](mailto:mghahramanafshar@nri.ac.ir)

How to cite this article: Esmailpour, M., & Ghahraman Afshar, M. (2023). Magnetic Nanoadsorbent: Preparation, characterization, and Adsorption Properties for Removal of Copper (II) from Aqueous Solutions. *Applied Chemistry Today*, **18(69)**, 11-20. (in Persian)

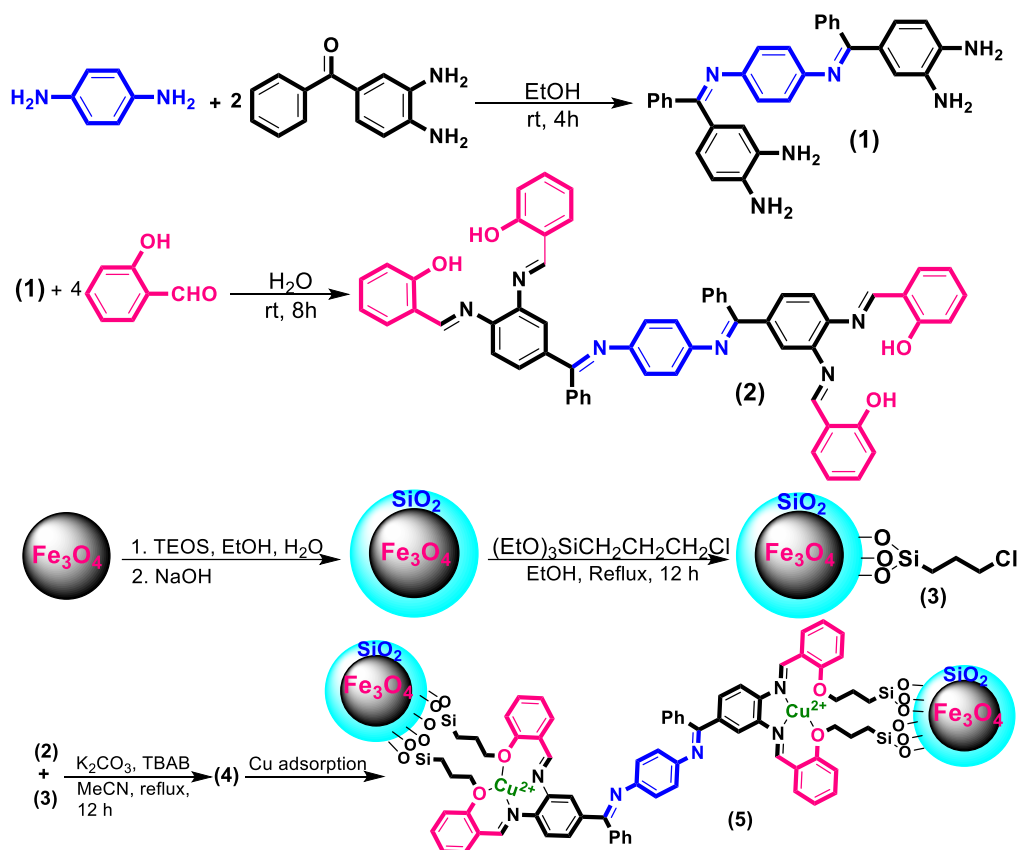
### 1. Introduction

Human activities such as urbanization, population increase, industrial and mining operations, in addition to unplanned, unscientific disposal methods, are the major contributing factors for rapid increase in the concentrations of heavy metal ions in the aquifers [1, 2]. Owing to their non-biodegradable feature, heavy metals can be accumulated in organisms through the food chain, causing various diseases and disorders [3, 4]. For instance,  $\text{Hg}^{2+}$  can cause brain disorders, nervous system damage, and kidney and endocrine system disruption [5, 6]. Cd (II) and Pb (II) are the most toxic and bio-persistent ions in drinking water, because of their use in plastic, steel and battery industries [7-9].

Also, copper can be noxious for ecological systems and also for human health. There are some other sicknesses attributed to overuse of copper including liver or kidney damage, intestinal disorders, and even cancer [10, 11]. Hence, the removal of heavy metal ions from water sources to an acceptable concentration is a current research challenge in water treatment and they are suitable as good pollutant model. Nowadays, a large number of approaches, such as ion exchange, flocculation, bioadsorption, membrane filtration, electrochemical, solvent extraction, precipitation and adsorption have been implemented for removing heavy metal and dye contaminants from wastewater [12]. However, some of these methods have difficulties with ions recovery, especially from high cost processes, generation of other waste products and dilute metal solutions [13]. Among these techniques, adsorption is the most attractive methods due to its high efficiency, simplicity and its ability to remove multiple heavy metals simultaneously [14].

In the recent years, nanomaterials have attracted more attention as a promising alternative adsorbent

in purifying wastewater contaminated with heavy metal ions owing to their unique features of a low diffusion resistance, size and surface effects, enhanced active sites and large specific surface area [15]. Magnetic nanoparticles such as  $\text{Fe}_3\text{O}_4$  MNPs are a kind of new nanomaterials that exhibits properties such as being superparamagnetism, lower toxicity and price, large surface area, chemical stability, high saturation magnetization, magnetic separation, uniform particle size distribution and enrichment biocompatibility [16]. However, raw MNPs are susceptible to air oxidation and leaching under acidic conditions, and are easily aggregated in aqueous solutions because of anisotropic dipolar attraction, which reduces the sorption capacity and restricts the application range [17]. To compensate for these shortages, a suitable coating on the surface of the pure magnetic nanoparticles is essential to avoid such limitations, meanwhile improves the physicochemical properties of the nanoparticles and maintains the colloidal suspension stability within the biological environment [18]. Therefore, silica-coated magnetic nanospheres have been subjected to extensive research, due to its stability, high surface area, easily tunability and economic availability [19]. Recently, a number of such functionalized  $\text{Fe}_3\text{O}_4@\text{SiO}_2$  nanoparticles have been employed in a range of applications [20]. Therefore, according to mentioned information, we decided to synthesis of bis-salophen Schiff base complex supported on  $\text{Fe}_3\text{O}_4@\text{SiO}_2$  MNPs as active agent for removing Cu(II) ions (Scheme 1). Then, the influences of adsorbent dosage, contact time on adsorption performance and kinetic behavior of  $\text{Fe}_3\text{O}_4@\text{SiO}_2/\text{Schiff}$  base MNPs were investigated for the removal of Cu(II) from aqueous solutions.



Scheme 1. Schematic representation of formation of  $\text{Fe}_3\text{O}_4@/\text{SiO}_2/\text{Schiff}$  base NPs.

## 2. Experimental procedure

### 2.1. Materials and physical measurements

All the chemical reagents were used as-received, without further purification. X-ray powder diffraction (XRD) analysis was conducted on a Bruker AXS D8-advance X-ray diffractometer using  $\text{Cu K}\alpha$  radiation ( $\lambda = 1.5418$ ). Fourier transform infrared (FT-IR) spectra were recorded in transmission mode with a Shimadzu FT-IR 8300 spectrometer.

Transmission electron microscopy (TEM) analysis was performed by using a Philips EM208 microscope operated at a 100 kV accelerating voltage. FE-SEM and EDX were performed on a Hitachi S-4160 instrument. The sample was sputtered by gold to avoid undesirable electron charging. VSM measurements were performed by using a vibrating sample magnetometer (BHV-55). The metal concentrations were measured with an inductively

coupled plasma spectrometer (ICP, analysis (Varian, Vista-pro).

### 2.2. General procedure

#### Preparation of $\text{Fe}_3\text{O}_4@/\text{SiO}_2$ NPs

$\text{Fe}_3\text{O}_4$  MNPs were prepared using a facile coprecipitation method. Silica was coated on the surface of  $\text{Fe}_3\text{O}_4$  MNPs via a modified Stöber sol-gel method [21]. In a typical process,  $\text{Fe}_3\text{O}_4$  MNPs (0.5 g) were added to an aqueous solution of ethanol (50 ml), deionized water (5 ml) and 5.0 ml of NaOH (10 wt.%). Finally, TEOS (0.2 ml) was added dropwise into the solution, which was stirred at room temperature for 30 min. After washing with water and ethanol several times, the isolated  $\text{Fe}_3\text{O}_4@/\text{SiO}_2$  MNPs were dried under vacuum at 80 °C for 10h.

#### General procedure for the preparation of $\text{Fe}_3\text{O}_4@/\text{SiO}_2$ MNPs functionalized with 3-chlorotriethoxypropylsilane ( $\text{Fe}_3\text{O}_4@/\text{SiO}_2\text{-Cl}$ )

$\text{Fe}_3\text{O}_4@/\text{SiO}_2$  MNPs (1 g) were dispersed in ethanol (20 ml) and sonicated for 10 min at room

temperature. Then, 3-chlorotriethoxypropylsilane (6 mmol) was introduced, and the mixture was stirred vigorously and refluxed for 12 h under nitrogen atmosphere. After refluxing, the mixture was cooled to room temperature, separated using an external magnet and washed thoroughly with ethanol and deionized water and dried in an oven at 60 °C to afford Fe<sub>3</sub>O<sub>4</sub>@SiO<sub>2</sub>-Cl MNPs [22].

#### **Synthesis of *p*-bis[(3,4-salicylicimino) benzophenimine (PSBP)]**

Benzene-1,4-diamine (1 mmol, 0.11 g) was dissolved in ethanol (15 ml) at room temperature. Then 3,4-diaminobenzophenone (2 mmol, 0.43 g) was added, and the mixture was stirred for 4 h. The purple solid crude product was filtered and then recrystallized from methanol to give pure PDBP. Then, PDBP (0.25 g, 0.5 mmol) and salicylaldehyde (0.25 g, 2 mmol) were added to 15 ml of water as a solvent, and the mixture was stirred at room temperature for 8 h. The dark yellow solid product (2, PSBP) was filtered and purified by recrystallization from methanol [22].

#### **Immobilization of bis-salophen Schiff base ligand on Fe<sub>3</sub>O<sub>4</sub>@SiO<sub>2</sub> MNPs**

Tetrabutylammonium bromide (TBAB, 0.02 g, 0.06 mmol) and K<sub>2</sub>CO<sub>3</sub> (4.0 mmol, 0.53 g) were added to 1 g of the former suspension of Fe<sub>3</sub>O<sub>4</sub>@SiO<sub>2</sub>-Cl nanoparticles in MeCN (15 mL) in the presence of PSPB (1.0 mmol) and the mixture was refluxed under constant stirring for 12 h. The residue was collected by a magnet, followed by washing several times with water and ethanol to unreacted species to obtain Fe<sub>3</sub>O<sub>4</sub>@SiO<sub>2</sub>/Schiff base.

### **3. Results and discussion**

#### **3.1. Characterization of bis-salophen Schiff base ligand on Fe<sub>3</sub>O<sub>4</sub>@SiO<sub>2</sub> MNPs**

FT-IR spectra of Fe<sub>3</sub>O<sub>4</sub>, Fe<sub>3</sub>O<sub>4</sub>@SiO<sub>2</sub>, Fe<sub>3</sub>O<sub>4</sub>@SiO<sub>2</sub>-Cl, PSBP and Fe<sub>3</sub>O<sub>4</sub>@SiO<sub>2</sub>/Schiff base are presented in Fig. 1. For all spectra, the symmetrical stretching vibration modes of O-H and deformation of adsorbed water molecules appear as a broad band

around 3200-3600 cm<sup>-1</sup> and a sharp band around 1620 cm<sup>-1</sup>, respectively. The band at 572 cm<sup>-1</sup> can be related to the absorption peak of Fe-O bond (Fig 1a). Fe<sub>3</sub>O<sub>4</sub>@SiO<sub>2</sub> structure has a strong band at about 3400 cm<sup>-1</sup> because of silanol-OH stretches on the surface of silica. Si-O stretches (asymmetric stretching) were observed with a strong band at about 1090 cm<sup>-1</sup> for all the silica coated compounds in the study (Fig 1b). Furthermore, the band at 791 cm<sup>-1</sup> is assigned to the Si-O-Si symmetric stretch (Fig 1b). The reaction of Fe<sub>3</sub>O<sub>4</sub>@SiO<sub>2</sub> and 3-chloromethoxypropylsilane and the formation of Fe<sub>3</sub>O<sub>4</sub>@SiO<sub>2</sub>-Cl NPs are confirmed by C-H (stretching), -CH<sub>2</sub>- (bending), and C-Cl (stretching) at 2955, 1443, and 702 cm<sup>-1</sup>, respectively, in the IR spectrum (Fig 1c). Characteristic bands of the C=N at 1651 cm<sup>-1</sup> (stretching vibration) and also the saturated C-H stretching vibrations at 2854-2923 cm<sup>-1</sup> demonstrate the successful synthesis of the PSBP molecule (Fig 1d). After the modification of Fe<sub>3</sub>O<sub>4</sub>@SiO<sub>2</sub>-Cl with PSBP, the appearance of new bands at 2857-2926, 1654 and 1436 cm<sup>-1</sup> correspond to C-H (stretching), C=N (stretching) and -CH<sub>2</sub>- (bending), respectively (Fig 1e). These results confirm that the adsorbent had been successfully prepared.

The structures of the Fe<sub>3</sub>O<sub>4</sub>, Fe<sub>3</sub>O<sub>4</sub>@SiO<sub>2</sub> and Fe<sub>3</sub>O<sub>4</sub>@SiO<sub>2</sub>/Schiff base nanoparticles were determined by powder X-ray diffraction (XRD). The position and relative intensities of all peaks confirm well with standard XRD pattern of Fe<sub>3</sub>O<sub>4</sub> (JCPDS card no. 01-1111) indicating retention of the crystalline cubic spinel structure. The pattern indicates a crystalline structure with peaks at 2θ= 30.1°, 35.4°, 43.1°, 53.4°, 57° and 62.6°, which are assigned to the (220), (311), (400), (422), (511) and (440) crystallographic faces of magnetite, consistent with the standard pattern (card no. 19-629) [19] (Fig. 2a) and also were observed for Fe<sub>3</sub>O<sub>4</sub>@SiO<sub>2</sub> and Fe<sub>3</sub>O<sub>4</sub>@SiO<sub>2</sub>/Schiff base NPs.

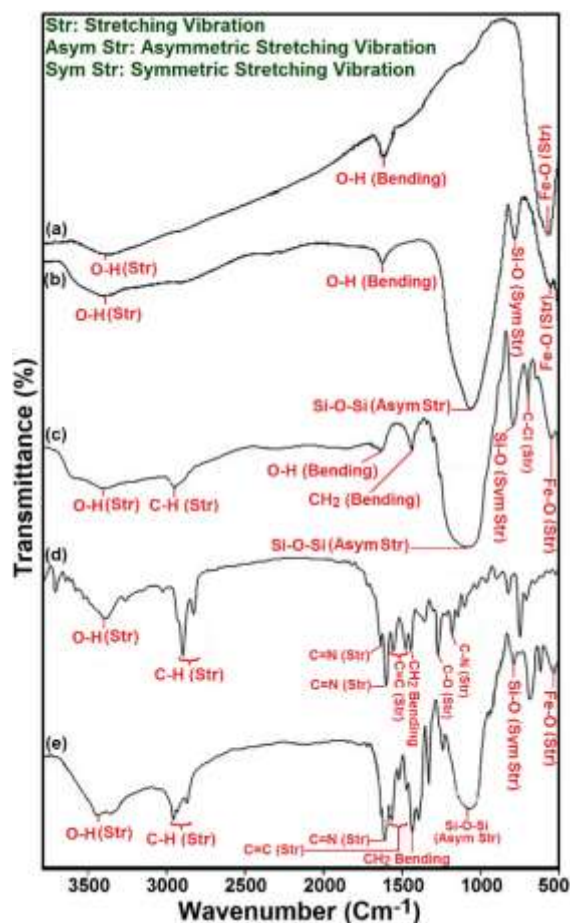


**Fig 1.** FTIR spectra of (a)  $\text{Fe}_3\text{O}_4$ , (b)  $\text{Fe}_3\text{O}_4@SiO_2$ , (c)  $\text{Fe}_3\text{O}_4@SiO_2\text{-Cl}$ , (d) PSBP and (e)  $\text{Fe}_3\text{O}_4@SiO_2/\text{Schiff}$  base (4) NPs.

This revealed that the surface modification of the  $\text{Fe}_3\text{O}_4$  nanoparticles does not lead to their phase changes. The XRD pattern of  $\text{Fe}_3\text{O}_4@SiO_2$  nanoparticles presented a broad featureless XRD peak at low diffraction angle ( $2\theta = 15\text{-}25^\circ$ ), which corresponded to the amorphous state silica shells (Fig. 2b). For  $\text{Fe}_3\text{O}_4@SiO_2/\text{Schiff}$  base ligand, the broad peak was transferred to lower angles due to the synergetic effect of amorphous silica and PSBP molecules (Fig. 2c).

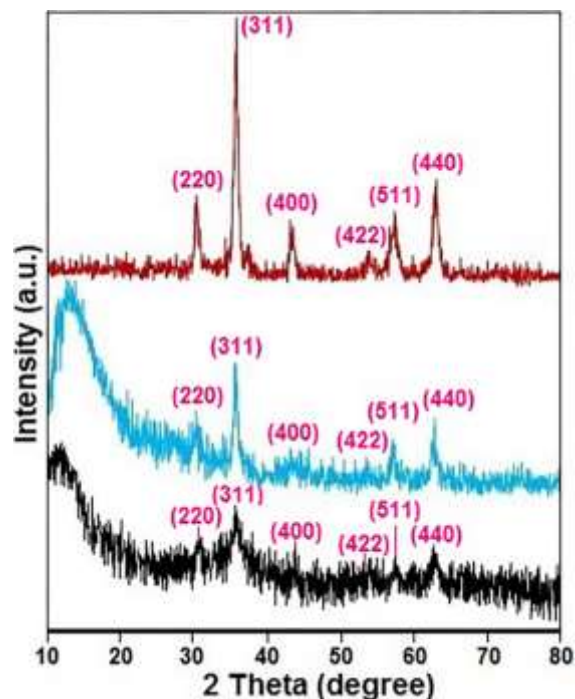


**Fig 2.** XRD patterns of (a)  $\text{Fe}_3\text{O}_4$  and (b)  $\text{Fe}_3\text{O}_4@SiO_2$  and  $\text{Fe}_3\text{O}_4@SiO_2/\text{Schiff}$  base NPs.

The morphology and sizes of  $\text{Fe}_3\text{O}_4$ ,  $\text{Fe}_3\text{O}_4@SiO_2$  and  $\text{Fe}_3\text{O}_4@SiO_2/\text{Schiff}$  base were observed by field emission scanning electron microscope (FE-SEM).  $\text{Fe}_3\text{O}_4$  nanoparticles are relatively monodisperse particles with an average diameter of about 15 nm (Fig. 3a).

As shown in Fig. 3b,  $\text{Fe}_3\text{O}_4$  nanoparticles with silica coating are approximately 20 nm. Chemical modification with schiff base ligand increases the nanoparticle size to 25 nm (Fig. 3c). To ascertain the composite morphology more clearly, the TEM images of the  $\text{Fe}_3\text{O}_4$ ,  $\text{Fe}_3\text{O}_4@SiO_2$  and  $\text{Fe}_3\text{O}_4@SiO_2/\text{Schiff}$  base nanocomposites are represented in Fig. 3d-f. The TEM image in Fig. 3d show that the  $\text{Fe}_3\text{O}_4$  nanoparticles have a mean diameter of about 15 nm and a nearly spherical shape. Based on the TEM images, the analysis of the  $\text{Fe}_3\text{O}_4@SiO_2$  and  $\text{Fe}_3\text{O}_4@SiO_2/\text{Schiff}$  base surface morphology demonstrated the agglomeration of many ultrafine particles with a diameter of about 20 and 25 nm, respectively (Fig. 3e, f).

The EDX elemental analysis is shown in Figure 4. From the spectrum, it can be seen that carbon,

nitrogen, oxygen, iron and Si elements present in the  $\text{Fe}_3\text{O}_4@/\text{SiO}_2/\text{Schiff}$  base sample which is in good agreement with the proposed adsorbent structure (Fig 4).

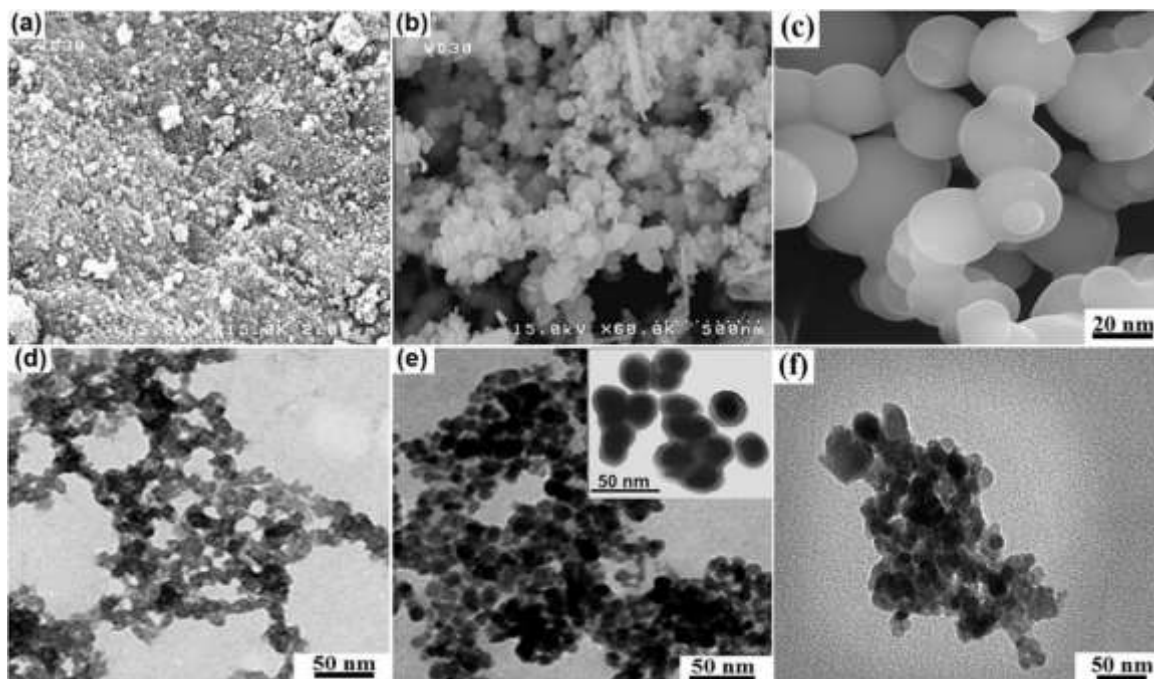


**Fig 3.** FE-SEM images of (a)  $\text{Fe}_3\text{O}_4$ , (b)  $\text{Fe}_3\text{O}_4@/\text{SiO}_2$  and (c)  $\text{Fe}_3\text{O}_4@/\text{SiO}_2/\text{Schiff}$  base NPs (b); TEM images of (d)  $\text{Fe}_3\text{O}_4$ , (e)  $\text{Fe}_3\text{O}_4@/\text{SiO}_2$  and (f)  $\text{Fe}_3\text{O}_4@/\text{SiO}_2/\text{Schiff}$  base NPs, respectively.

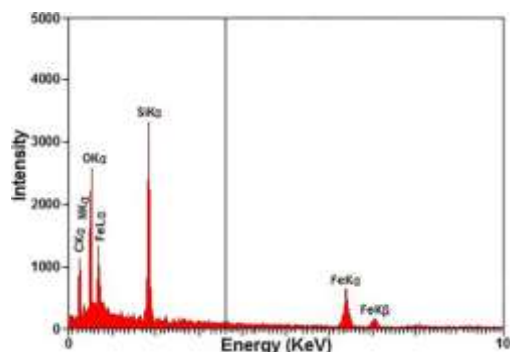


**Fig 4.** EDX analysis for  $\text{Fe}_3\text{O}_4@/\text{SiO}_2/\text{Schiff}$  base.

The magnetic properties of  $\text{Fe}_3\text{O}_4@/\text{SiO}_2/\text{Schiff}$  base nanocomposite was investigated using vibrating sample magnetometer (VSM) at room temperature in an applied magnetic field sweeping from -7 to 7 kOe.  $\text{Fe}_3\text{O}_4@/\text{SiO}_2/\text{Schiff}$  base nanocomposite exhibited superparamagnetism, presenting no remanence or coercitive forces (Fig. 5). The resultant magnetization saturation value of  $\text{Fe}_3\text{O}_4@/\text{SiO}_2/\text{Schiff}$  base was 29.87 emu/g, indicating strong magnetic response.

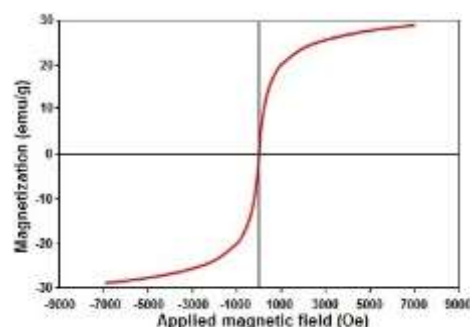


**Fig 5.** Room-temperature magnetic hysteresis loop of  $\text{Fe}_3\text{O}_4@/\text{SiO}_2/\text{Schiff}$  base NPs.

### 3.2. Effect of adsorbent dosage on Cu(II) ions adsorption

Adsorbent dosage is an important parameter because it determines the capacity of an adsorbent for a given initial concentration of the adsorbate. Adsorption of Cu(II) ions (initial concentration of 0.35 mmol/L) was studied using different dosages of  $\text{Fe}_3\text{O}_4@/\text{SiO}_2/\text{Schiff}$  base (3-24 mg) at the optimum pH (pH= 7) at 25 °C. As shown in Fig. 6a, percentage removal of copper ions enhances with the increase in adsorbent dosage. The maximum percent removal of all the studied copper ions was obtained with 21 mg



$\text{Fe}_3\text{O}_4@/\text{SiO}_2/\text{Schiff}$  base MNPs; this was, therefore, selected for further experiments.

### 3.3. Adsorption kinetics

The effect of contact time on the sorption of Cu(II) ions onto  $\text{Fe}_3\text{O}_4@/\text{SiO}_2/\text{Schiff}$  base containing 50 mL Cu(II) solution was investigated at initial concentration of 0.35 mmol/L and the results are

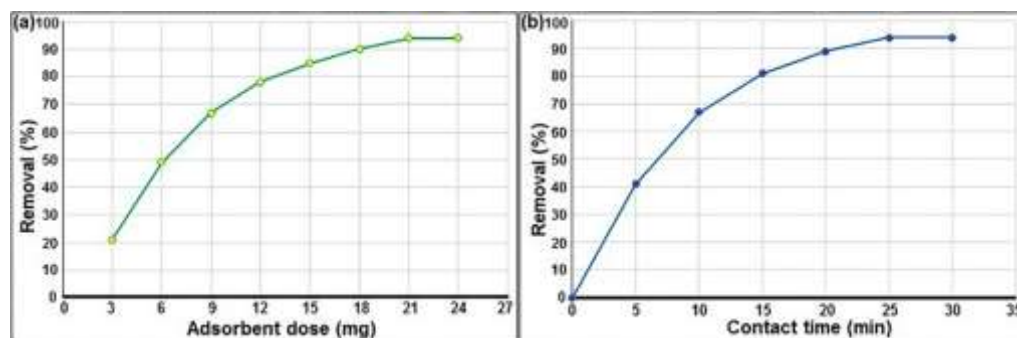


**Fig 6.** a) Effect of adsorbent dosage on the adsorption of Cu(II) ions by magnetic  $\text{Fe}_3\text{O}_4@/\text{SiO}_2/\text{Schiff}$  base NPs; b) Effect of contact time on the adsorption of Cu(II) ions by  $\text{Fe}_3\text{O}_4@/\text{SiO}_2/\text{Schiff}$  base NPs.

### 3.4. Desorption and reusability of $\text{Fe}_3\text{O}_4@/\text{SiO}_2/\text{Schiff}$ base ligand

The regeneration and repeated use of adsorbents is a crucial factor for assessing their potentials for practical applications. Therefore, sorption-desorption experiments were carried out six rounds

shown in Fig. 6b. The sorption of Cu(II) on  $\text{Fe}_3\text{O}_4@/\text{SiO}_2/\text{Schiff}$  base increases sharply within the first 5 min, then it rises slowly and reaches equilibrium within 25 min. As a result, the shaking time of 25 min was applied for Cu(II) adsorption by the magnetic bis-salophen schiff base ligand in subsequent steps.

in order to investigate the reusability of the prepared sorbents. The results show that the adsorbent shows a bit loss in adsorption capacity after six consecutive adsorption-desorption cycles and indicates the good performance and recyclability of the prepared  $\text{Fe}_3\text{O}_4@/\text{SiO}_2/\text{Schiff}$  base ligand as adsorbent.

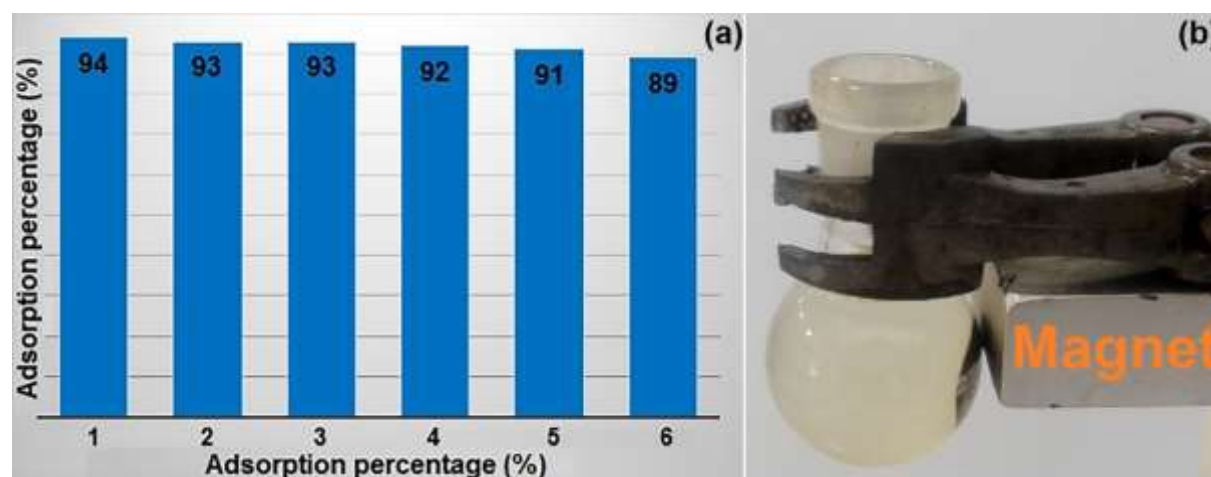


**Fig 7.** a) Adsorption efficiency of Cu(II) ions in the adsorption-desorption cycles by  $\text{Fe}_3\text{O}_4@/\text{SiO}_2/\text{Schiff}$  base MNPs at 25 °C; b) Photographs of the separation processes of  $\text{Fe}_3\text{O}_4@/\text{SiO}_2/\text{Schiff}$  base MNPs with external magnetic field.

## 4. Conclusion

A novel bis-salophen schiff base ligand supported on  $\text{Fe}_3\text{O}_4@/\text{SiO}_2$  nanoparticles was prepared and characterized.  $\text{Fe}_3\text{O}_4@/\text{SiO}_2/\text{Schiff}$  base NPs showed a rapid adsorption rate and a very high adsorption capacity for Cu(II) from aqueous medium. The

reactive functional of groups present on the surface of adsorbents and high surface-to-volume ratio of these nanoparticles provided more adsorption sites for metal ions. It seems that the magnetization of adsorbents and use of magnetic separation techniques can be an effective way to resolve problems

associated with separation and filtration. The practical test indicated that Fe<sub>3</sub>O<sub>4</sub>@SiO<sub>2</sub>/Schiff base was a reusable and efficient adsorbent, which was expected to can clean up more types of wastewater.

#### Acknowledgments

Authors gratefully acknowledge the financial support of this work by the Research Council of Payame Noor University of Estahban and Niroo Research Institute.

#### Conflicts of Interest

The author declares that there is no conflict of interest regarding the publication of this manuscript. In addition, the authors have entirely observed the ethical issues, including plagiarism, informed consent, misconduct, data fabrication and/or falsification, double publication and/or submission, and redundancy.

#### References

- [1] Wang, J. and Chen, C. (2009). Biosorbents for heavy metals removal and their future. *Biotechnology advances*, 27(2), 195-226.
- [2] Crespo, G.A., Afshar, M.G., Barrabés, N., Pawlak, M., and Bakker, E. (2015). Characterization of salophen Co (III) acetate ionophore for nitrite recognition. *Electrochimica Acta*, 179, 16-23.
- [3] Karaoğlu, M.H., Kula, I., and Uğurlu, M. (2013). Adsorption kinetic and equilibrium studies on removal of lead (II) onto glutamic acid/sepiolite. *CLEAN–Soil, Air, Water*, 41(6), 548-556.
- [4] Soleimani, M., Mahmodi, M.S., Morsali, A., Khani, A., and Afshar, M.G. (2011). Using a new ligand for solid phase extraction of mercury. *Journal of hazardous materials*, 189(1-2), 371-376.
- [5] Zhang, X. and Huang, J. (2010). Functional surface modification of natural

cellulose substances for colorimetric detection and adsorption of Hg<sup>2+</sup> in aqueous media. *Chemical Communications*, 46(33), 6042-6044.

- [6] Soleimani, M. and Afshar, M.G. (2015). Highly selective solid phase extraction of mercury ion based on novel ion imprinted polymer and its application to water and fish samples. *Journal of Analytical Chemistry*, 70(1), 5-12.
- [7] Kumar, M. and Puri, A. (2012). A review of permissible limits of drinking water. *Indian journal of occupational and environmental medicine*, 16(1), 40.
- [8] McAlary, T., Groenevelt, H., Disher, S., Arnold, J., Seethapathy, S., Sacco, P., Crump, D., Schumacher, B., Hayes, H., and Johnson, P.). *Environmental Science Processes & Impacts*.
- [9] Soleimani, M. and Afshar, M.G. (2014). Octaethylporphyrin as an ionophore for aluminum potentiometric sensor based on carbon paste electrode. *Russian Journal of Electrochemistry*, 50(6), 554-560.
- [10] Beppu, M., Arruda, E., Vieira, R., and Santos, N. (2004). Adsorption of Cu (II) on porous chitosan membranes functionalized with histidine. *Journal of Membrane Science*, 240(1-2), 227-235.
- [11] Pankratova, N., Crespo, G.A., Afshar, M.G., Crespi, M.C., Jeanneret, S., Cherubini, T., Tercier-Waeber, M.-L., Pomati, F., and Bakker, E. (2015). Potentiometric sensing array for monitoring aquatic systems. *Environmental Science: Processes & Impacts*, 17(5), 906-914.
- [12] Calagui, M.J.C., Senoro, D.B., Kan, C.-C., Salvacion, J.W., Futralan, C.M., and Wan, M.-W. (2014). Adsorption of indium (III) ions



from aqueous solution using chitosan-coated bentonite beads. *Journal of hazardous materials*, 277, 120-126.

[13] Alluri, H.K., Ronda, S.R., Settalluri, V.S., Bondili, J.S., Suryanarayana, V., and Venkateshwar, P. (2007). Biosorption: An eco-friendly alternative for heavy metal removal. *African Journal of Biotechnology*, 6(25).

[14] Njimou, J.R., Măicăneanu, A., Indolean, C., Nanseu-Njiki, C.P., and Ngameni, E. (2016). Removal of Cd (II) from synthetic wastewater by alginate–Ayous wood sawdust (Triplochiton scleroxylon) composite material. *Environmental Technology*, 37(11), 1369-1381.

[15] Xie, L., Jiang, R., Zhu, F., Liu, H., and Ouyang, G. (2014). Application of functionalized magnetic nanoparticles in sample preparation. *Analytical and Bioanalytical Chemistry*, 406(2), 377-399.

[16] Dindarloo Inaloo, I., Majnooni, S., Eslahi, H., and Esmaeilpour, M. (2020). Nickel (II) nanoparticles immobilized on EDTA-modified Fe<sub>3</sub>O<sub>4</sub>@ SiO<sub>2</sub> nanospheres as efficient and recyclable catalysts for ligand-free Suzuki–Miyaura coupling of aryl carbamates and sulfamates. *ACS omega*, 5(13), 7406-7417.

[17] Zong, P., Wang, S., Zhao, Y., Wang, H., Pan, H., and He, C. (2013). Synthesis and application of magnetic graphene/iron oxides composite for the removal of U (VI) from aqueous solutions. *Chemical Engineering Journal*, 220, 45-52.

[18] Zahmatkesh, S., Esmaeilpour, M., and Javidi, J. (2016). 1, 4-Dihydroxyanthraquinone–copper (II) supported on superparamagnetic Fe<sub>3</sub>O<sub>4</sub>@ SiO<sub>2</sub>: An efficient catalyst for N-arylation of nitrogen heterocycles and

alkylamines with aryl halides and click synthesis of 1-aryl-1, 2, 3-triazole derivatives. *RSC Advances*, 6(93), 90154-90164.

[19] Esmaeilpour, M., Sardarian, A.R., and Firouzabadi, H. (2018). N-heterocyclic carbene-Pd (II) complex based on theophylline supported on Fe<sub>3</sub>O<sub>4</sub>@ SiO<sub>2</sub> nanoparticles: Highly active, durable and magnetically separable catalyst for green Suzuki-Miyaura and Sonogashira-Hagihara coupling reactions. *Journal of Organometallic Chemistry*, 873, 22-34.

[20] Peng, X., Xu, F., Zhang, W., Wang, J., Zeng, C., Niu, M., and Chmielewska, E. (2014). Magnetic Fe<sub>3</sub>O<sub>4</sub>@ silica–xanthan gum composites for aqueous removal and recovery of Pb<sup>2+</sup>. *Colloids and Surfaces A: Physicochemical and Engineering Aspects*, 443, 27-36.

[21] Vibhute, S.P., Mhaldar, P.M., Shejwal, R.V., Rashinkar, G.S., and Pore, D.M. (2020). Palladium schiff base complex immobilized on magnetic nanoparticles: an efficient and recyclable catalyst for Mizoroki and Matsuda-Heck coupling. *Tetrahedron Letters*, 61(17), 151801.

[22] Sardarian, A.R., Kazemnejadi, M., and Esmaeilpour, M. (2019). Bis-salophen palladium complex immobilized on Fe<sub>3</sub>O<sub>4</sub>@ SiO<sub>2</sub> nanoparticles as a highly active and durable phosphine-free catalyst for Heck and copper-free Sonogashira coupling reactions. *Dalton Transactions*, 48(9), 3132-3145.